Optimizing performance of half-metals at finite temperature

Attema, J. J.; de Wijs, G. A.; de Groot, R. A.

Published in:
Journal of Physics-Condensed Matter

DOI:
10.1088/0953-8984/19/31/315212

IOP PUBLISHING JOURNAL OF PHYSICS: CONDENSED MATTER

J. Phys.: Condens. Matter **19** (2007) 315212 (14pp) doi:10.1088/0953-8984/19/31/315212

Optimizing performance of half-metals at finite temperature

J J Attema[1], G A de Wijs[1] and R A de Groot[1,2]

[1] Electronic Structure of Materials, IMM, Radboud University Nijmegen, Toernooiveld 1, 6525 ED Nijmegen, The Netherlands
[2] Laboratory for Chemical Physics, Zernike Institute for Advanced Materials, University of Groningen, Nijenborgh 4, 9747 AG Groningen, The Netherlands

E-mail: R.deGroot@science.ru.nl

Received 7 November 2006, in final form 10 May 2007
Published 3 July 2007
Online at stacks.iop.org/JPhysCM/19/315212

Abstract

Several aspects of half-metallic magnetism at finite temperature are discussed. Since NiMnSb is the simplest half-metal and the longest known it will be used as an example. Also it is a half-metal with remarkable little on-site Coulomb repulsion. Consequently it is a half-metal that is not notably corrupted by non-quasiparticle states. There exists an anomaly at 90 K, described before, that will be shown to be unrelated to the position of the Fermi level in the bandgap. Several substitutions are investigated that could shed some light on the origin of the transition. The calculated phonon spectrum is compared with experimental neutron scattering data. Finally, the spin-polarization of interfaces of NiMnSb with the transition metal based non-magnetic semiconductors NiTiSn and CoTiSb is investigated and the electronic structure of an infinite two-dimensional array of NiMnSb quantum dots embedded in NiScSb is reported.

1. Introduction

Half-metallic magnetism was discovered almost a quarter of a century ago (de Groot *et al* 1984). Its importance for applications nowadays referred to as 'spintronics' was realized from the beginning (de Groot *et al* 1983). Experimental realizations have proven to be more problematic; part of the problem is that surfaces and interfaces often turn out to be more complex than was assumed in the early days. Another complication is temperature.

There are two fundamental reasons why 100% spin-polarization of a half-metal can only be approached. The first is the spin–orbit coupling that mixes states of the two spin directions. The strength of the spin–orbit interaction is basically an atomic property and scales with the fourth power of the nuclear charge. How much depolarization results given the strength of the spin–orbit interaction is very much dependent on details of the bandstructure: it is for example very small for NiMnSb because of the free electron-like behaviour of the metallic

charge carriers in the vicinity of the Fermi level. If the remaining spin–orbit coupling is still problematic, the only alternative is the application of half-metals based on lighter elements than 3d transition metals (Attema *et al* 2005). The second source of depolarization is temperature. The thermal excitation of magnons leads to mixing of the two spin directions giving a reduction of the spin-polarization with increasing temperature until the polarization vanishes at the Curie point. There are several possibilities for influencing the magnon spectrum in order to reduce the depolarizing effects of magnons. One way is to increase the magnetic anisotropy, since this will reduce the number of thermally available magnon states by the introduction of gaps in the magnon bandstructure at the Γ-point. Another strategy is the introduction of impurities with minimal effect on the electronic structure, but maximal influence on the magnon structure. The (partial) substitution of a trivalent element like scandium for manganese in NiMnSb will leave the bandgap for the minority-spin direction unaffected. But since it lacks the magnetic moment of the manganese it replaces, the random suppression of magnetic moments will transform the continuous magnon spectrum into the discrete spectrum of an amorphous system (Attema *et al* 2004). A similar result is obtained by the application of the half-metal in the form of nano-dots. This strategy will be treated in the present paper.

All these considerations are valid for half-metals in general. A problem that is possibly specific for NiMnSb is a phase transition at about 90 K (Hordequin *et al* 2000). Although specific details of this transition are not completely clear yet, there are indications that half-metallic properties at that temperature are being lost. One possibility is a feedback mechanism (Hordequin *et al* 2000), in which thermal excitations from the top of the valence band of the minority spin direction to (majority) states at the Fermi energy cause an avalanche effect. Other suggestions are that the transition is connected to some form of disorder of the small magnetic moment on the nickel, leading to a loss of the half-metallic properties (Borca *et al* 2001), the loss of the magnetic moment on nickel in the case of disorder (Ležaić *et al* 2006), the reduction of both manganese and nickel moments (Borca *et al* 2001) or is related to magnon–phonon interaction (Dowben and Skomski 2003). The situation is far from clear, partially because measurements on thin layers (Moodera and Mootoo 1994, Borca *et al* 2001) give different results from measurements of bulk samples (Otto *et al* 1989b, 1989a).

Calculations will be presented in order to investigate whether partial substitution for nickel can suppress the spin disorder. Another aspect is the influence of so-called non-quasiparticle states. These states are predicted to occur theoretically (Irkhin and Katsnelson 2006). Although several possibilities for detecting these states have been suggested, at present there is no experimental confirmation of their existence. However, the non-quasiparticle states could be important at interfaces. Frequently, an interface of a half-metal with, for example, a semiconductor will not be half-metallic. This is not expected to be a problem as long as this interface is thin enough, thinner than the spin-flip scattering length. Nevertheless, the influence of the interface is often much stronger than expected. A possible explanation is that the interaction between non-quasiparticle states—present throughout the half-metal, but not carrying a current—and quasiparticle states—confined to the interface—could lead to a situation where conduction for the semiconducting spin direction is possible over a much longer distance. Careful measurements of the temperature dependence of the transport properties of interfaces could elucidate this point. It will be shown that they have a small influence in NiMnSb, which is therefore a true quasiparticle half-metal, even at non-zero temperature.

2. The origin of the bandgap in NiMnSb

The origin of the bandgap for the minority-spin direction was explained in strict analogy with III–V semiconductors, where the manganese in the half-metal plays the role of the trivalent

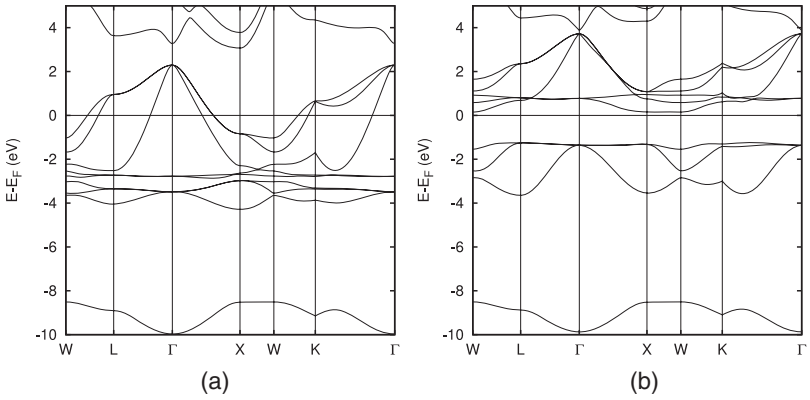

Figure 1. Bandstructure of MnSb in the zincblende structure for (a) the majority-spin direction and (b) minority-spin direction. The overall topology is similar as in NiMnSb.

metal in the semiconductor. The role of the nickel is to mediate the interaction between the tri- and pentavalent species, to insure a tetrahedral coordination for both manganese and antimony *and* to realize this in a stable crystal structure (de Groot *et al* 1984). This explanation does suggest that the MnSb in the zincblende structure should show a similar bandstructure to NiMnSb. This is actually the case: figure 1 shows the bandstructure of MnSb at the calculated equilibrium lattice parameter of 618 pm. That nickel is very efficient in stabilizing MnSb in the Heusler structure is dramatically exemplified by the fact that the *addition* of a nickel atom into zincblende MnSb *reduces* the equilibrium lattice parameter to the 591 pm in the resulting Heusler $C1_b$ phase. This clearly shows the importance of proper optimization of equilibrium lattice parameters. The overall bandstructure of MnSb in the zincblende structure is similar to that of NiMnSb. Differences are, of course, the absence of the nickel d-states and the flatness of the top of the valence band and bottom of the conduction band due to the larger equilibrium lattice parameter of MnSb in the zincblende structure.

Several attempts to explain the occurrence of the bandgap in NiMnSb on the basis of the nickel and manganese atoms alone have been published (Nanda and Dasgupta 2003, Galanakis *et al* 2002). Since these calculations remove the antimony while keeping the lattice parameters fixed, the analyses are based on highly inflated lattices. As a matter of fact, the experimental volume of existing Ni–Mn (Buschow *et al* 1983) is more than a factor of 2 smaller than that of NiMnSb. Such a procedure can lead to bandgaps for reasons differing from those pertaining to the real half-metal. Illustrative examples are found in the alkali metals. With increasing lattice parameter they undergo a transition to a magnetic phase and eventually to a Mott insulating state. Thus a half-metallic solution induced by the inflation of the lattice alone is perfectly possible. This was actually demonstrated for lithium quite some time ago (Min *et al* 1986). There are no indications that lithium is a half-metallic ferromagnet under equilibrium conditions.

In the first paper on half-metallic NiMnSb the similarity between NiMnSb and zincblende GaSb was illustrated by the similarity in bandstructure and thus interactions (Slater and Koster 1954) obscured by the nickel d-states. It is of importance to notice that the figure caption in figure 2 '*where Ni d-states were deliberately removed from the Hamiltonian*' (de Groot *et al* 1984) did not mean to imply that the mediating role of them in bridging the manganese antimony interaction was excluded as well (this could have been stated more explicitly).

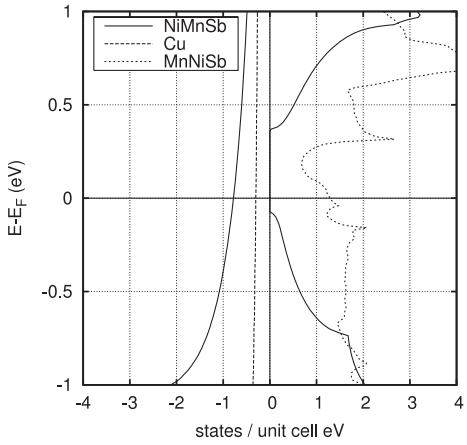

Figure 2. Density of states for majority-spin NiMnSb (negative ordinate, full line), minority-spin NiMnSb (positive ordinate, full line), non-magnetic copper (negative ordinate, broken) and NiMnSb minority spin with identical Ni and Mn lattices but antimony and empty sites interchanged (positive ordinate, broken line).

If the nickel–manganese pair were sufficient to explain the bandgap in NiMnSb, the position of the antimony is irrelevant by definition. The contrary is the case, however. Figure 2 shows the density of states of NiMnSb in the (incorrect) crystal structure as determined by Webster and Mankikar (1984) as well as in the correct structure. The manganese and nickel lattices are identical, but the antimony and the empty site are interchanged. No bandgap occurs for the incorrect structure. Half-metallic ferromagnetism occurs only in the case that the antimony adjoins a nickel atom and not in the case when antimony is coordinated by manganese (Helmholdt *et al* 1984). Actually, the density of states for NiMnSb with antimony and an empty site interchanged shows an electronic structure very different from genuine NiMnSb, with many Van Hove singularities in a small panel around the Fermi energy. The interactions responsible for the bandgap in NiMnSb were probably best summarized by Kübler: 'a nickel induced manganese–antimony covalent interaction' (Kübler 2000).

This is in line with the detrimental effects of disorder. Even 1% interchange suffices to suppress the half-metallic properties (Orgassa *et al* 2000). The original explanation of the bandgap for the minority-spin direction in NiMnSb incorporates all these aspects in a natural way. It should be noted that the cases of disorder detrimental to the half-metallic properties in NiMnSb are thermodynamically the most unlikely ones (Attema *et al* 2004).

3. NiMnSb: a true quasiparticle half-metal

The Fermi energy in a half-metal is determined by the metallic spin direction. So, no excitations are expected to be possible in the semiconducting spin direction for energies smaller than the distance between the top of the valence band and the Fermi energy. However, in higher order these excitations can take place as a combination of excitations in the metallic spin direction and virtual magnons (Edwards and Hertz 1973, Irkhin and Katsnelson 2006). The resulting states are called non-quasiparticle (incoherent) states. This many-body process requires a finite Hubbard U. For small Hubbard U the resulting spectral weight of the non-quasiparticle (NQP) states is proportional to U, it saturates for U between 1 and 2 eV (Chioncel *et al* 2003). A Hubbard U can be calculated in principle, but in practice it is treated as an empirical parameter.

So it is in order to discuss the values of the Hubbard Us appropriate for half-metals and in particular for NiMnSb. Earlier work has assumed *ad hoc* a value of U of 2 eV: the purpose of it was not so much to give a quantitatively correct calculation of the NQP states in NiMnSb, but to compare the theoretically expected general spectral features of the NQP with those calculated for an actual material. NiMnSb was chosen because it is the simplest of all half-metals (cubic symmetry with three atoms per primitive unit cell only).

But NiMnSb is an unusual material in many respects. The excitement over the occurrence of a bandgap (for one spin direction exclusively) overshadowed the equally unusual electronic structure for the metallic (majority) spin direction in NiMnSb. The density of states curves for the two spin directions of high accuracy are shown in figure 2. The bandgap for the minority-spin direction is evident, but we focus on the majority-spin direction here. It shows a low, structureless density of states, free of any Van Hove singularities in a panel of several electron-volts around the Fermi energy. This is an unusual situation for a transition metal compound. Of all elemental solids, it resembles most the density of states of copper (also shown in figure 2). One wonders what the value of the Hubbard U will be for NiMnSb.

A direct experimental determination of U is possible by means of Auger spectroscopy. To the best of our knowledge such measurements have not been reported. Another way to determine the Hubbard U is in comparing density functional calculations with photoemission measurements. The position of a one-electron level in density functional theory depends on the occupation of that level. The occupation of the level clearly changes in the photoemission process. Since the energy of a one-electron level is given in density functional theory as the partial derivative of the total energy of the system to the occupation of the level under consideration, the second derivative of the total energy with respect to the occupation of the one-electron level gives the dependence of the position of the one-electron level on its occupation. The second derivative of the total energy is a very good approximation of the Hubbard U. In other words, it is expected that calculated one-electron levels deviate from photoemission measurements, where the deviations are given by the Hubbard Us. There is one caveat, however. Deviations should not be introduced by additional approximations *within* density functional theory like the use of atomic spheres or neglect of spin–orbit interactions. The first one is negligible for a cubic system with high packing ratio and the latter one is discussed below.

Besides the early work with spin-resolved photoemission measurements by Bona *et al* (1985) focusing on the spin-polarization at threshold, work has been reported by Robey *et al* (1992) as well as Kang *et al* (1995). Unfortunately, these measurements were neither angular nor spin-resolved and were performed on polycrystalline samples only. This is a serious drawback, since photoemission spectra are very surface sensitive, particularly for some of the excitation energies employed by the latter two groups. The surface electronic structure of NiMnSb deviates from that of the bulk. It is not half-metallic. Several phenomena are responsible for this. First of all, without special precautions, the surface of NiMnSb is very easily oxidized; leading to a chemical composition different from that of the bulk and the chance that the half-metallic properties will be maintained is vanishingly small. But without special care even a non-oxidized surface shows segregation with loss of the half-metallic properties (Ristoiu *et al* 2000, Caruso *et al* 2003, Panchula *et al* 2003, Jenkins 2004). On the other hand, spin-polarized photoemission measurements on carefully sputtered and annealed polycrystalline NiMnSb resulted in a spin-polarization of 40% half an electron-volt below threshold (Zhu *et al* 2001). This is much larger than the polarization derived from magnetoresistance data (Tanaka *et al* 1997). As explanation for the deviations from 100% the presence of another phase and/or a lower surface magnetization was suggested. In addition, we remark that even the non-oxidized surface of the proper stoichiometry is not half-metallic

because the origin of the half-metallicity in Heusler $C1_b$s requires an unperturbed zincblende like structure with tetrahedral coordinated manganese and antimony atoms (de Wijs and de Groot 2001, Attema *et al* 2006). This situation is violated at the surface.

The most detailed information is obtained from angle-resolved photoemission on single crystals. The first such measurements on a half-metal were the work of Kisker *et al* (1987) on PtMnSb rather than NiMnSb. The fact that PtMnSb was used rather than NiMnSb is only a minor complication since both compounds are isostructural as well as isoelectronic, and their calculated bandstructures are very similar. The main difference is caused by the relativistic mass–velocity and Darwin terms: the occurrence of a M_0 Van Hove singularity originating from the bottom of the conduction band at Γ. In NiMnSb the position of this singularity is higher in energy, above the panel of figure 2.

This is reflected in the actual measurements. The integrated measurements of Robey *et al* show a signal just below the Fermi energy that seems to be inconsistent with a half-metallic ferromagnet. But since the surface of PtMnSb is not expected to be half-metallic, it is dangerous to draw conclusions for the bulk here. On the other hand, the angle-resolved measurements of Kisker *et al* show a very good agreement with the calculated bandstructure. The largest systematic disagreement between the measured and calculated bandstructures is at the top of the valence band around the gamma point for the minority-spin direction. This is a direct consequence of the spin–orbit interaction. While the *strength* of the spin–orbit interaction is an almost atomic property (it varies with the fourth power of the nuclear charge), its *impact* on the actual bandstructure is very much dependent on the material and the k vector. A maximal effect is obtained there where the orbit angular momentum is degenerate. This is exactly the case for the top of the valence band at the Γ-point. The size of the disagreement is in perfect agreement with what is expected for the strength of the spin–orbit interaction in PtMnSb (de Groot and Buschow 1986). The remaining disagreements between the measured photoemission data and the calculated dispersions are a direct measure of the Hubbard U. From this comparison we expect a Hubbard U of 0 ± 0.1 eV for PtMnSb.

Recently, angle-resolved photoemission measurements were performed on NiMnSb (Correa *et al* 2006). The authors compared their measurements with calculated spectra and judged the comparison as 'not satisfying yet'. However, the one band which was detected is in remarkably good agreement with the highest band of the majority-spin direction not intersecting the Fermi level, both in the topology (dispersion) and in the absolute position, with a typical accuracy of 0.1 eV. Also, the fact that the detected band coincides with the electron-band with the least dispersion may not be coincidental. The influence of spin–orbit interaction at the Γ-point is negligible here compared with PtMnSb. This primarily reflects the fact that, unlike the situation in PtMnSb, the state at the Γ-point for the majority-spin direction is doubly degenerate and shows very strong orbital quenching (it consists of one eigenvalue with $m_l = 0$ and another *one* with a linear combination of $m_l = \pm 2$ states). In order to allow for spin–orbit coupling, we need an admixture of the bridging $m_l = \pm 1$ states as well as the other $m_l = \pm 2$ state, which are all higher in energy. Another reason is that the contribution of nickel to the spin–orbit interaction is smaller than that of the heavier platinum.

So, there is strong evidence that both NiMnSb and PtMnSb have a Hubbard U of the order of 0.1 eV. This implies that, at finite temperatures, the influence of non-quasiparticle states in NiMnSb is negligible compared with the effect of thermally excited magnons. These Heusler alloys have the property of showing dominantly quasiparticle behaviour at *any* temperature. This is quite unique. Other Heusler $C1_b$ half-metals like FeMnSb show bandstructures for the metallic spin direction much more in line with what one expects for transition metal compounds: less dispersive bands and several Van Hove singularities in the vicinity of the Fermi level. This trend is even stronger in half-metals in the $L2_1$ structure. Half-metallic oxides

like CrO_2, the colossal magnetoresistance materials and magnetite are even more localized. The latter is even a Mott insulator at low temperatures.

4. The 90 K anomaly

As mentioned in the introduction, a phase transition is likely to take place around 90 K in NiMnSb. The exact nature is not clear, partially because of conflicting experiments and partially because of a lack of understanding. Two possible effects are discussed here. The first one is the influence of the position of the Fermi energy with respect to the bandgap.

A position of the Fermi level just above the top of the valence band or below the bottom of the conduction band forms a potential source of instability in a half-metal. Assuming a bandgap for the minority-spin direction, as is the case for the majority of half-metals, thermal excitations from the top of the valence band are possible to the majority-spin channel at the Fermi energy. These excitations increase the magnetic moment, leading to an increase in the exchange splitting. This implies a lowering of the majority-spin bands with respect to the minority bands. Thus successive excitations require increasingly less energy. This positive feedback results in a collapse of the half-metallic properties. On the other hand, if the Fermi energy is close to the bottom of the minority-spin conduction band, the situation is reversed. Thermal excitations are now from the majority-spin channel at the Fermi energy to the minority-spin conduction band and they decrease the magnetic moment. This, in turn, lowers the exchange splitting and raises the majority-spin bands, and again results in a positive feedback. This phenomenon occurs for all possible cases independently of whether the bandgap is for the minority or majority spins or whether the Fermi level approaches the valence or conduction band. The effectiveness of this mechanism depends on the position of the Fermi energy at zero temperature but also strongly depends on the density of states at the Fermi energy for the metallic spin direction, as well as the density of states at the top of the valence band or the bottom of the conduction band (whichever is closest to the Fermi energy).

Suppose the Fermi level is positioned asymmetrically in the gap, so the influence of either valence or conduction band can be neglected. Assume that the density of states at the metallic spin direction is N and that at the semiconducting spin direction it is zero within the gap and also N elsewhere. The transfer of charge δ by thermal excitation increases the exchange splitting by $2\delta I$, where I is the exchange interaction. This shift is offset by a change in band energy of $2\delta/N$. So a positive feedback is possible only if the effect of the exchange splitting dominates, which leads to a Stoner-like criterion $NI > 1$. This should not be confused with the 'real' Stoner criterion; it gives the condition under which *thermal excitations* can lead to a collapse of the half-metallic properties and thus could be named the 'dynamic Stoner criterion'. We focus our attention again on figure 2. Not only are the densities of states low, but the variations with energy are also remarkably slow. Thus the effect of thermal excitations is very unlikely to be the origin of the 90 K anomaly. We will return to this point later.

The magnetic moment in NiMnSb is mainly carried by the manganese. However, a small moment is found on the nickel. Since several studies link the transition to a disordering of the nickel moment, possibly connected with a loss of the moment altogether, we will investigate the possibility of substitutions on the nickel lattice in order to influence the transition. It is therefore useful to consider the situation in related Heusler $C1_b$ compounds. Isoelectronic PtMnSb is also half-metallic, but here the magnetic moment is just confined to the manganese sublattice. It would be interesting to investigate whether PtMnSb undergoes a similar transition, in which case the transition is a property of the manganese sublattice only. PdMnSb is not half-metallic, the Fermi level intersects the valence band just below the minority spin bandgap. CoMnSb on the other hand is calculated to be half-metallic with a total moment of 3 μ_B (Kübler 1984).

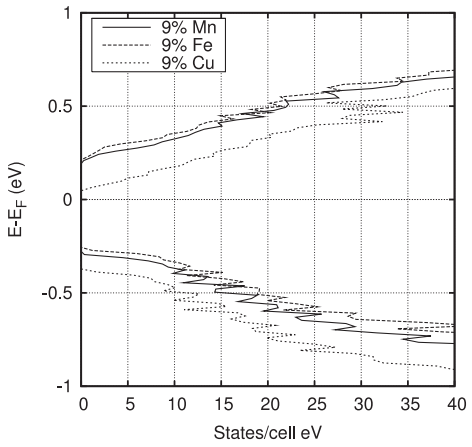

Figure 3. Density of states of (a) $Ni_{0.91}Cu_{0.09}MnSb$ for the minority-spin direction (dotted line), (b) $Ni_{0.91}Fe_{0.09}MnSb$ (broken line) and (c) $Ni_{0.91}Mn_{1.09}Sb$ (full line).

Experimentally, a compound with this composition exists, but it adopts a distorted structure with partial occupation of the cobalt on the empty sites in the pristine $C1_b$ structure. The experimentally determined magnetic moments are inconsistent with a half-metallic electronic structure. The next step is FeMnSb. This is a promising candidate: if it were to be a half-metal it should have a magnetic moment of 2 μ_B, which it actually has (de Groot *et al* 1986): the moments of the iron and manganese sublattices order antiferromagnetically with respect to each other, leading to 2 μ_B as the difference of the local moments. Experimentally, the situation is more complex, however. FeMnSb exists, but its crystal structure is similar to CoMnSb and consequently it is not half-metallic. However, partial substitution of nickel by iron is possible and the crystal structure remains the genuine $C1_b$ one up to 10% of iron. This really looks promising. Suppose the 90 K anomaly is due to a weakness of the coupling of the magnetization of the nickel sublattice to the magnetization of the manganese sublattice. Substitutions on either lattice may influence this coupling, either by introducing an antiferromagnetic coupling, or by strengthening a ferromagnetic coupling. Since the manganese sublattice is responsible for the high Curie temperature, substitutions on the nickel sublattice are preferred. Also, the substitutions should be sufficiently stable to make them realizable in practice. Of course, the prime consideration is whether these substitutions will preserve the half-metallic properties.

Substitutions of copper, iron and manganese for nickel were investigated using the LSW method (Van Leuken *et al* 1990) as well as extra nickel on the empty position in the $C1_b$ structure. The introduction of 9% copper leads to a half-metallic solution with the Fermi energy at the bottom of the conduction band (figure 3(a)). The bandgap is reduced to 0.37 eV (undoped: 0.45 eV). The magnetic moment is increased to 4.09 μ_B per formula unit, located on the nickel and manganese atoms (this non-integral magnetic moment is not in conflict with the half-metallic properties here since it pertains to a formula unit rather than a unit cell). Substitution of 25% of the nickel by copper still shows a bandgap of 0.26 eV but the Fermi energy is located in the conduction band and the half-metallic properties were lost. Figure 3(b) shows the density of states of NiMnSb with a 9% substitution of the nickel by iron. It is clear that the half-metallic properties are preserved. The magnetic moments on manganese are not affected on the average, while the moments on the nickel are somewhat reduced. Its moments are ordered parallel to the manganese moments, while iron carries a small moment of 0.75 μ_B antiparallel to the other magnetic species. The bandgap is reduced to 0.42 eV. Even

the substitution of 25% of the nickel (that cannot be realized experimentally while maintaining the Heusler $C1_b$ structure) does not lead to the reversal of the nickel magnetization. Figure 3(c) shows the influence of the replacement of 9% of the nickel by manganese. The bandgap is 0.43 eV, practically the same as the undoped system. The Fermi energy is located in the middle of the bandgap. The moments of manganese and nickel are hardly affected at all, manganese at the nickel site orders antiferromagnetically with a moment of 2.1 μ_B. A substitution of 25% leads to a similar results with a small reduction of the nickel moments, still parallel to the manganese magnetization. Finally, we consider the introduction of an extra nickel on the empty position in the $C1_b$ structure. The density of states is very similar to the undoped system. The bandgap is reduced to 0.31 eV. The extra nickel is practically non-magnetic and the magnetic moments of the atoms in the pristine structure are hardly affected. Unfortunately, the magnetic moments of the nickel atoms are still ordered parallel to those of the manganese atoms.

None of the substitutions is able to alter the sign of the coupling between the manganese and nickel sublattices at zero temperature. The robustness of this coupling is somewhat surprising in view of the fact that a thermal energy of just 90 K might break it. A valid question is whether the size of this coupling is modified in a useful way. It is clear that the substitution with copper will not work. Even if it enhances the strength of the coupling between the two magnetic sublattices (which is not to be expected), the increase in the density of states for the majority-spin direction to 1 state/eV and the position of the Fermi level close to the bottom of the conduction band introduces a source of thermal instability possibly worse than in the undoped system. The substitution with iron, and in particular manganese, looks attractive. It introduces sizable moments on the sublattice so it is unimaginable that this will not influence the coupling one way or another. The density of states at the Fermi energy for the majority-spin direction has also increased to 1 state/eV, but the Fermi energy is located in the middle of the bandgap.

The substitution of iron is experimentally proven to be stable. No data are available for $Ni_{1-x}Mn_{1+x}Sb$ to the best of our knowledge. This compound can be thought of as an alloy of the two existing (hence stable) compounds NiMnSb and Mn_2Sb. From the total energy of the three compounds it follows that the substitution of a manganese for a nickel costs 45 meV. The effect of entropy at a typical annealing temperature should be sufficient to stabilize the substituted compound for small concentrations.

5. Phonons in NiMnSb

For several reasons knowledge and understanding of phonons is important. Even at zero temperature phonons have an influence on the physical properties of a system through the effects of zero point motion. At finite temperature the phonon spectrum determines thermodynamic functions. Anomalies in phonon spectra can explain lattice instabilities and phase transitions. Finally, it has been suggested that the 90 K anomaly in NiMnSb may be due to phonon–magnon interactions (Dowben and Skomski 2003). Accurate measurements of the phonon (and magnon) spectra NiMnSb were carried out by Hordequin *et al* (1996) and Borca *et al* (2000). In this paragraph we will compare the calculated phonon spectrum with experimental data.

First-principles phonon calculations have been carried out with the Vienna *ab initio* simulation programme (VASP) (Kresse and Hafner 1993, Kresse and Furthmüller 1996). Using the projector augmented wave method (Blöchl 1994, Kresse and Joubert 1999). Density functional theory within the generalized gradient approximation was used (Perdew *et al* 1992). The phonon frequencies were obtained employing a direct method (Kresse *et al* 1995). Calculations were carried out in a periodically repeated simple cubic supercell ($a = 1182.6$ pm)

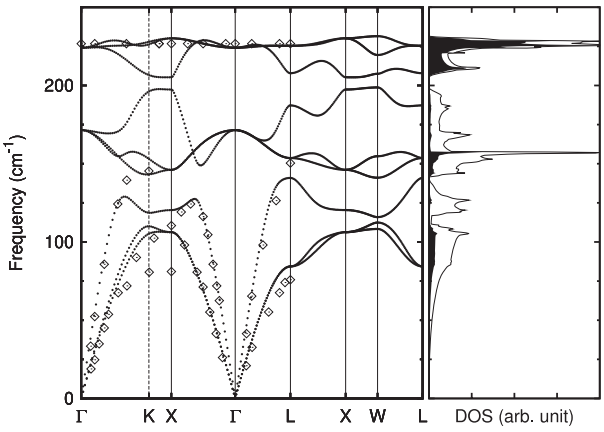

Figure 4. Calculated phononic bandstructure compared with the experimental points of Borca *et al* (2000). The vertical scale is in reciprocal centimetres. Right-hand panel: integrated total phonon density of states (line). The contribution of nickel is indicated in black.

containing 32 formula units. In the supercell a Ni, Sb or a Mn atom was displaced 5 pm from its lattice position and the resulting forces on all 96 atoms calculated. Thus the interatomic force constant matrix was constructed. Subsequently eigenfrequencies were obtained by diagonalization of the dynamical matrix.

The Brillouin zone of the supercell was sampled on a $4 \times 4 \times 4$ k-point grid. A Gaussian Fermi smearing of 0.2 eV was applied.

Figure 4 shows the calculated phonon branches as well as the partial nickel and total densities of states. The experimental points are indicated with diamonds. In general a good agreement between calculations and experiment exists. The agreement is less at the zone boundaries, most notably for the K and X points. Excellent agreement exists for the optical modes at 225 cm^{-1}. From the comparison with the calculated spectrum, it is remarkable that only dispersionless optical branches are detected experimentally. This is partially explained by the eigenfunctions associated with the various phonon modes. In interpreting the eigenfunctions it has to be kept in mind that the cross-sections for scattering in NiMnSb are dominated by the contribution of the nickel-lattice (www.ncnr.nist.gov/resources/n-lengths/). At the Γ point the eigenvector of the highest triplet is dominated by displacements of the nickel atom, while the lower triplet at ∼175 cm^{-1} shows displacements on the antimony and manganese lattices. The latter branch has not been observed experimentally. At the X point the highest (doublet) state is also determined by the nickel sublattice, in line with the fact that this mode is observed. The singlet state somewhat lower in energy is not observed, however, in spite of its nickel character. This may be related to its more dispersive character. The other singlet state around 200 cm^{-1} at the X point originates primarily from the manganese and antimony lattices. The doublet at ∼150 cm^{-1} has a mixed character. The lowest three branches are characterized by displacements on the manganese and antimony lattices. Both are experimentally observed, but with a remarkable large discrepancy up to 25 cm^{-1}. At the L point, the lowest doublet is of mixed character and is observed; the acoustical singlet is not observed at the L point, but its dispersion can be traced along the Γ–L line. The observed doublet at ∼150 cm^{-1} is of manganese–antimony character. The higher unobserved singlets are of manganese/antimony and nickel character in order of increasing energy, respectively, while the highest (doublet) state is of mixed character, with a slight nickel dominance. The

latter state is observed. So, in general a good agreement is obtained, with as exception the acoustical branches at the X and K point. We have no explanation for this.

Phonon–magnon coupling has been suggested as a possible explanation for the 90 K anomaly. On the basis of the phonon spectrum alone it is not possible to make definite statements on the importance of phonon–magnon coupling. In the original paper (Dowben and Skomski 2003), the intersection of the very steep magnon mode with the phonon mode at 225 cm^{-1} was considered. We also found a mode at $\sim$180 cm^{-1} that could be a candidate for magnon–phonon interactions. The frequency is in line with the temperature of the transition. What is different is the eigenvector of the phonon mode.

But magnon–phonon interactions also depend on the derivative of the strength of the interatomic exchange coupling with respect to distance. *A priori* it seems unlikely that this derivative is large in view of the high Curie temperature of NiMnSb, the highest of all Heusler $C1_b$ compounds. This is not a rigorous proof, however, since the Curie temperature depends on more than one exchange coupling only.

6. The spin-polarization of half-metallic nano-dots

The prime source of the reduction of the spin-polarization of the conduction electrons in NiMnSb is magnon excitations. It can be advantageous to replace a macroscopic contact with an array of nanoscopic quantum dots. This way the continuous magnon spectrum of a macroscopic contact can be replaced by a discrete spectrum of the nano-dots. The size of the dots and their spacing can be optimized for maximal spin-polarization at a specific temperature (Attema *et al* 2004). This way the spin-polarization can be improved at moderate temperatures. No miracles should be expected, however, at higher temperatures, say beyond half the Curie temperature. A serious complication is that none of the surfaces of NiMnSb are half-metallic, so without precautions, a negligible fraction of a quantum dot will actually be half-metallic. A solution to this problem is to embed the quantum dots in a suitable matrix. The embedding material should be insulating (or at least semiconducting) and show half-metallic interfaces with NiMnSb for all possible interfaces, or at least all interfaces of low index. Thus traditional main-group semiconductors like CdSe or InP cannot be used here. They show genuinely half-metallic (111) interfaces, but all other interfaces cannot be half-metallic because they posses anion coordination by a mixture of main group and transition metals (Attema *et al* 2006). Thus the only alternative is the use of semiconductors based on transition metals. Three of them have been considered: NiScSb, NiTiSn and CoTiSb. They have different advantages and disadvantages. NiScSb has the advantage that it introduces one new element (Sc) *only*, but the lattice mismatch is the largest of the three semiconductors (2.1%). NiTiSn shows the smallest bandgap, but also the smallest lattice mismatch with NiMnSb (0.2%).

Interfaces between NiMnSb and NiScSb have been studied before; the interfaces of lowest index were shown to conserve the half-metallic properties (Attema *et al* 2004). Here we concentrate on the interfaces with NiTiSn and CoTiSb. Both compounds were studied by Tobola *et al* (1998). The bandstructure of NiTiSn is shown in figure 5; we refer to Tobola *et al* (1998) for the bandstructure of CoTiSb. Calculations were performed using the LSW method (Van Leuken *et al* 1990). In figure 6 we show the density of states for the (110) interface between NiMnSb and NiTiSn, it is clearly half-metallic. The (100) interface shows a similar density of states. However, the (111) interface is *not* half-metallic due to the presence of tin-derived states being pushed down from the conduction band. For this reason NiTiSn will not be considered further. The (100), (110) and (111) interfaces between NiMnSb and CoTiSb conserve the half-metallic properties completely. Of course, the ultimate test for the preservation of half-metallic properties at the interface is the calculation of an actual quantum

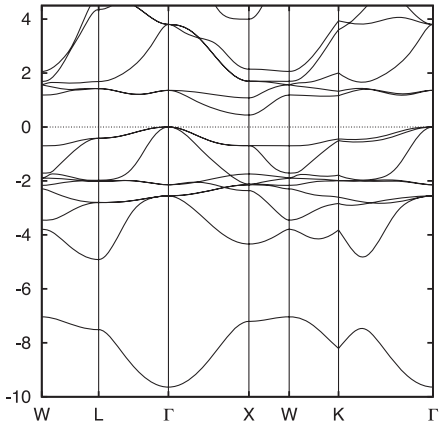

Figure 5. The bandstructure of NiTiSn.

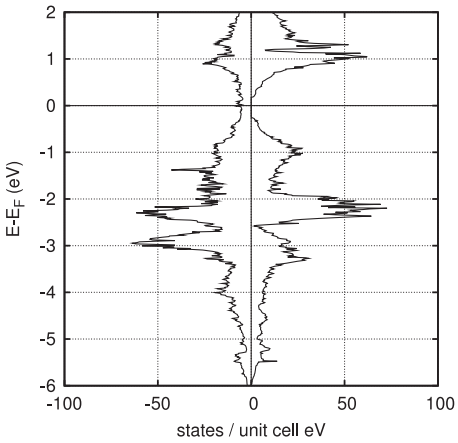

Figure 6. Density of states of a (110) interface between the half-metal NiMnSb and the non-magnetic semiconductor NiTiSn.

dot. In figure 7 we show the density of states of a two-dimensional array of quantum dots of NiMnSb. Each unit consists of 16 conventional units of NiScSb, the quantum dot is obtained by replacing the four central units by NiMnSb. Periodicity is used in the third direction. The conclusion of figure 7 is that it is possible indeed to have nanoscopic dots of a half-metal that remain completely half-metallic even in the case of NiMnSb, provided the dots are embedded in a suitably chosen matrix. The study of the physical properties of this system at finite temperature is under way.

7. Conclusions

Various explanations for the occurrence of the bandgap in half-metallic Heusler $C1_b$ alloys have been considered. Recent explanations based on a nickel–manganese interaction alone have to be rejected in favour of the original explanation, in strict analogy with III–V semiconductors.

The influence of non-quasiparticle states on properties at finite temperature of both NiMnSb as well as PtMnSb was found to be negligible in view of the small Hubbard Us

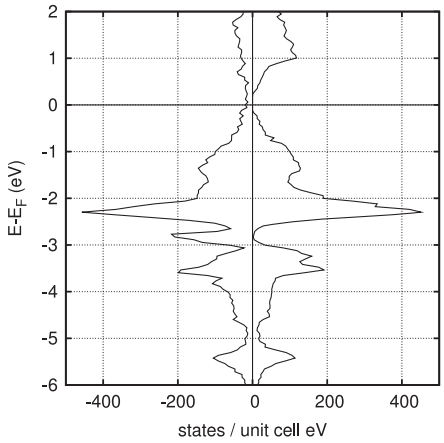

Figure 7. Density of states of a two-dimensional array of quantum dots of NiMnSb embedded in NiScSb. The half-metallic properties are conserved.

determined by the comparison of angle-resolved photoemission spectra with density functional calculations.

The 90 K anomaly in NiMnSb has been considered. It seems unlikely that it is connected with a special position of the Fermi level with respect to the bandgap, since this explanation requires a high density of states near the Fermi energy, while these are exceptionally low and structureless in NiMnSb. Experimental work on PtMnSb could show if the anomaly is purely a feature of the manganese sublattice or if it is caused by the disordering of the nickel moments. If the latter, substitution of nickel with either manganese or iron could have a positive effect on the transition.

Calculated phonon spectra have been compared with measured ones and on the whole a good agreement was observed.

Finally several possibilities for the realization of spin-injection from half-metallic nano-dots have been investigated. Genuine half-metallic nano-dots can be realized by embedding in suitable chosen semiconductors, NiScSb and possibly CoTiSb, based on transition-metals.

Acknowledgments

This work is part of the research programme of the 'Stichting voor Fundamenteel Onderzoek der Materie', which is financially supported by the 'Nederlandse Organisatie voor Wetenschappelijk Onderzoek (NWO)'. Contributions from 'Nanoimpuls' and 'Nanoned' through the Technology Foundation (STW) are also acknowledged.

References

Attema J J, de Wijs G A, Blake G R and de Groot R A 2005 *J. Am. Chem. Soc.* **127** 16325

Attema J J, de Wijs G A and de Groot R A 2006 *J. Phys. D: Appl. Phys.* **39** 793

Attema J J, Fang C M, Chioncel L, de Wijs G A, Lichtenstein A I and de Groot R A 2004 *J. Phys.: Condens. Matter* **16** s5517

Blöchl P E 1994 *Phys. Rev.* B **50** 17953

Bona G L, Meier F, Taborelli M, Bucher E and Schmidt P H 1985 *Solid State Commun.* **56** 391

Borca C N, Komesu T, Jeong H-K, Dowben P A, Hordequin Ch, Nozieres J P, Pierre J, Stadler S and Idzerda Y U 2001 *Phys. Rev.* B **64** 052409

Borca C N, Komesu T, Jeong H-K, Dowben P A, Ristoiu D, Hordequin Ch, Pierre J and Nozieres J P 2000 *Appl. Phys. Lett.* **77** 88
Buschow K H J, Van Engen P G and Jongbreur R 1983 *J. Magn. Magn. Mater.* **38** 1
Caruso A N, Borca C N, Ristoiu D, Nozieres J P and Dowben P A 2003 *Surf. Sci. Lett.* **525** L109
Chioncel L, Katsnelson M I, de Groot R A and Lichtenstein A I 2003 *Phys. Rev.* B **68** 144425
Correa J S, Eibl Ch, Rangelov G, Braun J and Donath M 2006 *Phys. Rev.* B **73** 125316
de Groot R A and Buschow K H J 1986 *J. Magn. Magn. Mater.* **54–57** 1377
de Groot R A, Janner A G M and Mueller F M 1983 *Patents* NL19830000602, EP198402000215 etc
de Groot R A, Mueller F M, van Engen P G and Buschow K H J 1984 *Phys. Rev. Lett.* **50** 2024
de Groot R A, van der Kraan A M and Buschow K H J 1986 *J. Magn. Magn. Mater.* **61** 330
de Wijs G A and de Groot R A 2001 *Phys. Rev.* B **64** 0204402
Dowben P A and Skomski R 2003 *J. Appl. Phys.* **93** 7948
Edwards D M and Hertz J A 1973 *J. Phys. F: Metal Phys.* **3** 2191
Galanakis I, Dederichs P H and Papanikolaou N 2002 *Phys. Rev.* B **66** 134428
Helmholdt R B, de Groot R A, Mueller F M, van Engen P G and Buschow K H J 1984 *J. Magn. Magn. Mater.* **43** 249
Hordequin C, Pierre J and Currat R 1996 *J. Magn. Magn. Mater.* **162** 75
Hordequin C, Ristoiu D, Ranno L and Pierre J 2000 *Eur. Phys. J.* B **16** 287
Irkhin V Yu and Katsnelson M I 2006 *Phys. Rev.* B **73** 104429
Jenkins S J 2004 *Phys. Rev.* B **70** 245401
Kang J S, Park J G, Olson C G, Youn S J and Min B I 1995 *J. Phys.: Condens. Matter* **7** 3789
Kisker E, Carbone C, Flipse C F and Wasserman E F 1987 *J. Magn. Magn. Mater.* **70** 21
Kresse G and Furthmüller J 1996 *Phys. Rev.* B **54** 11169
Kresse G, Furthmüller J and Hafner J 1995 *Europhys. Lett.* **32** 729
Kresse G and Hafner J 1993 *Phys. Rev.* B **47** 558
Kresse G and Joubert D 1999 *Phys. Rev.* B **59** 1758
Kübler J 1984 *Physica* B+C **127** 257
Kübler J 2000 *Theory of Itinerant Electron Magnetism* (Oxford: Oxford University Press)
Ležaić M, Mavropoulos P, Enkovaara J, Bihlmayer G and Blügel S 2006 *Phys. Rev. Lett.* **97** 026404
Min I, Oguchi T, Jansen H J F and Freeman A J 1986 *Phys. Rev.* B **33** 324
Moodera J S and Mootoo D M 1994 *J. Appl. Phys.* **76** 6101
Nanda B R K and Dasgupta I 2003 *J. Phys.: Condens. Matter* **15** 7307
Orgassa D, Fujiwara H, Schulthess T C and Butler W H 2000 *J. Appl. Phys.* **87** 5870
Otto M J, van Woerden R A M, van der Valk P J, Wijngaard J, van Bruggen C F and Haas C 1989a *J. Phys.: Condens. Matter* **1** 2351
Otto M J, van Woerden R A M, van der Valk P J, Wijngaard J, van Bruggen C F, Haas C and Buschow K H J 1989b *J. Phys.: Condens. Matter* **1** 2341
Panchula A F, Kaiser C, Kellock A and Parkin S P 2003 *Appl. Phys. Lett.* **83** 1812
Perdew J P, Chavary J A, Vosko S H, Jackson K A, Pederson M R, Singh D J and Fiolhais C 1992 *Phys. Rev.* B **46** 6671
Ristoiu D, Nozieres J P, Borca C N, Borca B and Dowben P A 2000 *Appl. Phys. Lett.* **76** 2349
Robey S W, Hudson L T and Kurtz R L 1992 *Phys. Rev.* B **46** 11697
Slater J C and Koster G F 1954 *Phys. Rev.* **94** 1498
Tanaka C T, Nowak J and Moodera J S 1997 *J. Appl. Phys.* **81** 5515
Tobola J, Pierre J, Kaprzyk S, Skolozdra R V and Kouacou M A 1998 *J. Phys.: Condens. Matter* **10** 1013
Van Leuken H, Lodder A, Czyżyk M T, Springelkamp F and de Groot R A 1990 *Phys. Rev.* B **41** 5613
Webster P J and Mankikar R M 1984 *J. Magn. Magn. Mater.* **42** 300
Zhu W, Sinkovic B, Vescovo E, Tanaka C and Moodera J S 2001 *Phys. Rev.* B **64** 060403